13th Australasian Fluid Mechanics Conference
Monash University, Melbourne, Australia
13-18 December 1998

REYNOLDS NUMBER EFFECTS ON WALL-BOUNDED TURBULENCE

Alexander J. SMITS, David R. WILLIAMS,
and Michael A. SCHMANSKE*

Department of Mechanical and Aerospace Engineering
Princeton University, Princeton, NJ 08544, U.S.A.

ABSTRACT

Preliminary measurements of turbulence are reported for fully-developed turbulent pipe flow over a very wide Reynolds number range. The data were obtained in the Princeton/DARPA/ONR Superpipe facility which uses compressed air at pressures up to 240 atmospheres as the working fluid. The measurements include the longitudinal turbulence intensity, space-time correlations, and structure angle data. The Reynolds number ranges from 30×10^3 to 8.0×10^6, which is at least one order-of-magnitude higher than previously measured.

INTRODUCTION

The behavior of turbulence at high Reynolds number is interesting from a fundamental point of view, in that most theories of turbulence make very specific predictions in the limit of infinite Reynolds number. From a more practical point of view, there exist many applications that involve turbulent flow where the Reynolds numbers are extremely large. For example, large vehicles such as submarines and commercial transports operate at Reynolds numbers based on length of the order of 10^9, and industrial pipe flows cover a very wide range of Reynolds numbers up to 10^7. Some typical values are given in table 1, where Re_ℓ is Reynolds number based on length given by

$$Re_\ell = \frac{\rho U_\infty \ell}{\mu} = \frac{U_\infty \ell}{\nu},$$

where ρ is the density, ℓ is the length, U_∞ the speed, μ is the dynamic viscosity and ν is the kinematic viscosity. Similarly, Re_δ is based on U_∞ and the expected maximum value of the boundary layer thickness, Re_D is based on the average velocity $\bar{U}$ and the pipe diameter, and

$$Re_\tau = \frac{D u_\tau}{\nu},$$

where u_τ is the friction velocity ($= \sqrt{\tau_w/\rho}$, τ_w is the shear stress at the wall). The examples listed in table 1 are of engineering interest, but very important applications pertain to atmospheric and other geophysical flows where extremely high Reynolds numbers are the rule rather than the exception.

	$Re_\ell \times 10^{-6}$	$Re_\delta \times 10^{-5}$
Submarine	1000	700
Aircraft carrier	2500	1400
Boeing 747	560	400

	$Re_D \times 10^{-6}$	$Re_\tau \times 10^{-5}$
Water main	60	15
Natural gas main	40	10

Table 1: Typical Reynolds numbers encountered in practice.

To model the behavior of high Reynolds number turbulence it is often necessary to extrapolate laboratory results obtained at considerably smaller Reynolds numbers. This scaling process is fraught with uncertainty, even for relatively simple flows such as pipe flows. Here, we present some observations regarding the Reynolds number dependence of turbulent pipe flows. The mean flow scaling has been considered by Zagarola & Smits (1997, 1998a). Here, we focus on the turbulence behavior.

EXPERIMENT

Turbulence measurements were obtained in the Princeton/DARPA/ONR Superpipe apparatus which can achieve a range of Reynolds numbers spanning three orders-of-magnitude. The facility uses compressed air as the working fluid to achieve very high Reynolds numbers at a reasonable cost. A closed-loop system was built with the test pipe located inside high-pressure piping (see figure 1). The test pipe had a nominal diameter of 129 mm, with a length-to-diameter ratio of 200. Further details of the facility are given in Zagarola (1996) and Zagarola & Smits (1997).

*Susquehanna Investment Company, Chicago, IL

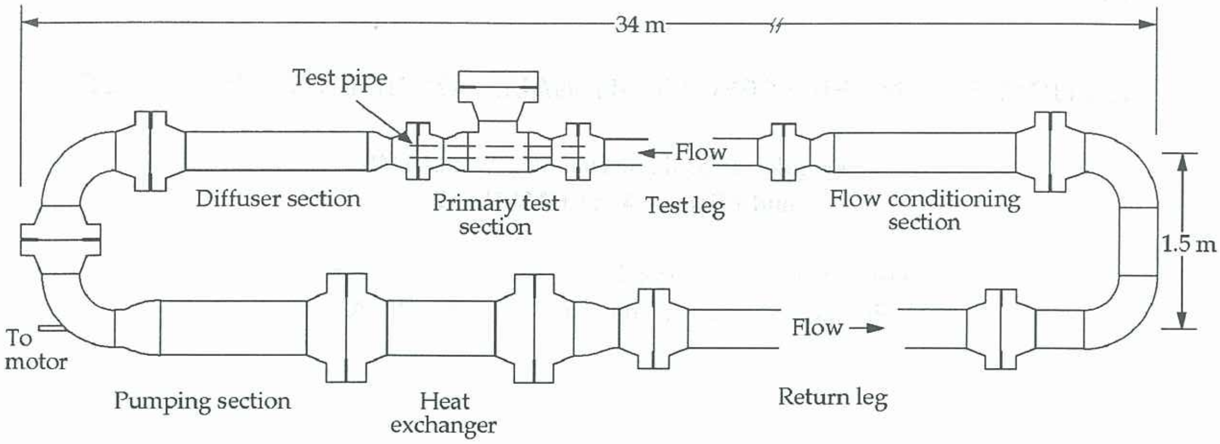

Figure 1: The layout of the SuperPipe facility. The flow direction is counter-clockwise.

Turbulence measurements were made using normal hot wires operated in the constant temperature mode using standard DANTEC equipment. The wires were calibrated by fitting a third-order polynomial to the velocity-voltage data, as recommended by Perry (1982). The high mass-flow rates in the pipe often produced frequency responses in excess of 600 kHz, even with $5\mu m$ diameter tungsten wires. The principal limitation on the hot-wire response was due to spatial averaging. The wire lengths were typically 0.8 to 1.0 mm long. At the highest Reynolds numbers, the spatial averaging led to a significant underestimate of the turbulence intensity, especially for locations near the wall. This filtering effect was estimated using the work of Wyngaard (1968) and the underestimation of $\overline{u'^2}$ is summarized in table 2.

Re_D	$y = 0.05R$	$y = R$
30.1×10^3	-3%	-2%
121×10^3	-3%	-3%
502×10^3	-5%	-3%
2.08×10^6	-7%	-3%
4.02×10^6	-7%	-5%
8.01×10^6	-10%	-5%

Table 2: Estimated maximum uncertainty in measurements of $\overline{u'^2}$ due to spatial filtering at two y-distances. R is the radius of the pipe.

The wall-normal distance y was set using a linear stepper motor with a resolution of 0.002 mm. The uncertainty in the initial position was ± 0.016 mm, so that the total uncertainty in y was always better than ± 0.05 mm.

The data acquisition system had a maximum sampling rate of 1 MHz per channel. Spectra were measured using three sampling frequencies: high (0.5 or 1 MHz), medium (25 or 50 KHz), or low (1.25 or 2.5 kHz). A low-pass filter set at half the maximum sampling frequency was used to reduce aliasing problems. No high-pass filter was used. Instead, the DC component of the hot-wire signal was reduced by subtracting off using a known offset voltage.

Space correlations, and space-time correlations were measured using two normal hot wires with constant spacing in the y-direction. The spacing was fixed at 5 mm. Particular attention was paid to match the frequency response of the two wires to minimize errors due to phase delays. The structure angle α was determined using the time delay to the maximum of the space-time correlation τ_{max}, the spacing between the wires ξ_y, and the convection velocity of the large-scales U_c (taken to be equal to the mean velocity at the average y-position). That is:

$$\tan\alpha = \frac{\xi_y}{\tau_{max} U_c}.$$

For the structure angle the main source of the error is in finding the position of the maximum in the space-time correlation.

RESULTS AND DISCUSSION

The results for the broadband turbulence intensities are shown in figure 2.

Near the wall, the high levels of turbulence are evident, but the filtering effect of the limited spatial resolution precludes any definite conclusions regarding the Reynolds number dependence of, say, the peak turbulence intensity. The outer layer behavior is more conclusive, and it appears that for $y/R \geq 0.1$ the turbulence intensities "saturate" for Reynolds numbers greater than about 120,000.

A very rough basis for comparison between pipe

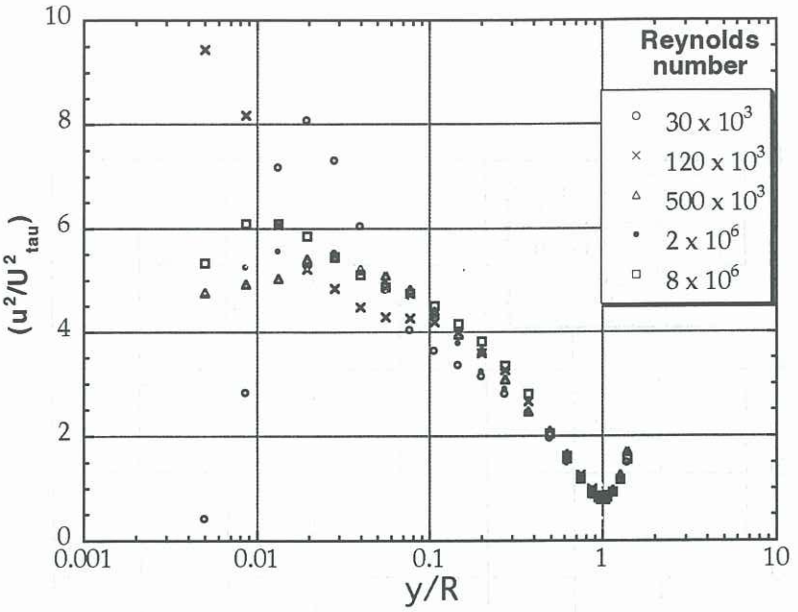

Figure 2: Turbulence intensity profiles normalized using outer scaling variables.

and boundary layer flows is to estimate the ratio of the largest to the smallest scale. For fully-developed pipe flow this ratio is given by Du_τ/ν (where we choose the diameter rather than the radius to characterize the large scales), and for a boundary layer it is $\delta u_\tau/\nu$. On this basis, the saturation limit ($Re_D = 120,000$) for the pipe flow is given by $Du_\tau/\nu =$ 5,660. If we assume that the equivalent boundary layer has $\delta u_\tau/\nu =$ 5,660, which gives $\theta U_\infty/\nu \approx$ 15,000. This is well beyond the point where the wake component of a turbulent boundary layer becomes independent of Reynolds number, and it is at the limit of what is possible in most laboratory experiments in boundary layers. However, comparisons between boundary layers and pipe flows must be made very carefully. Even though a similar scaling may exist for boundary layers and pipe flow, we can not expect the functional form of the velocity profiles in the outer region $g(\eta)$ to be the same since the equations of motion and the boundary conditions are different. This is true even in the infinite Reynolds number limit. Furthermore, any limit that depends on Reynolds number may be different due to the differences in the outer region.

The structure angle values are shown in figures 3 and 4. The Reynolds number dependence is interesting in that a definite trend to lower angles is seen for Reynolds numbers up to 300,000, which then reverses toward higher angles at higher Reynolds numbers. A similar trend toward lower structure angles was observed by Smith (1994) in a boundary layer. Smith noted a 10° decrease in the angle as the momentum thickness Reynolds number increased from 5,000 to 13,000. The highest Reynolds number obtained by Smith corresponds to a pipe flow Reynolds number of about 100,000 (if we use the ratio of the largest to the smallest scales as the appropriate parameter for comparison), which is still in the lower half of the Reynolds numbers studied in the pipe flow experiment, where we also observe a decrease in structure angle.

ACKNOWLEDGEMENT

The research in high Reynolds number flows is supported by ONR through grants N000014-92-J-1796, N000014-97-1-0618, and N000014-98-1-0325, monitored by Dr. L.P. Purtell.

REFERENCES

PERRY, A.E.,*Hot-wire Anemometry*, Oxford University Press, 1982.

SMITH, R.W, *Effect of Reynolds number on the structure of turbulent boundary layers*, Ph.D. Thesis, Princeton University, Princeton, NJ, 1994.

WYNGAARD, J. C., "Measurement of small-scale turbulence structures with hot-wires", *J. Sci. Instruments,* **1**, Series 2, 1968.

ZAGAROLA, M.V., *Mean flow scaling in turbulent pipe flow,* Ph.D. Thesis, Princeton University, 1996.

ZAGAROLA, M.V. and SMITS, A.J., "Scaling of the mean velocity profile for turbulent pipe flow", *Physics Review Letters,* **78** (2), 239–242, 1997.

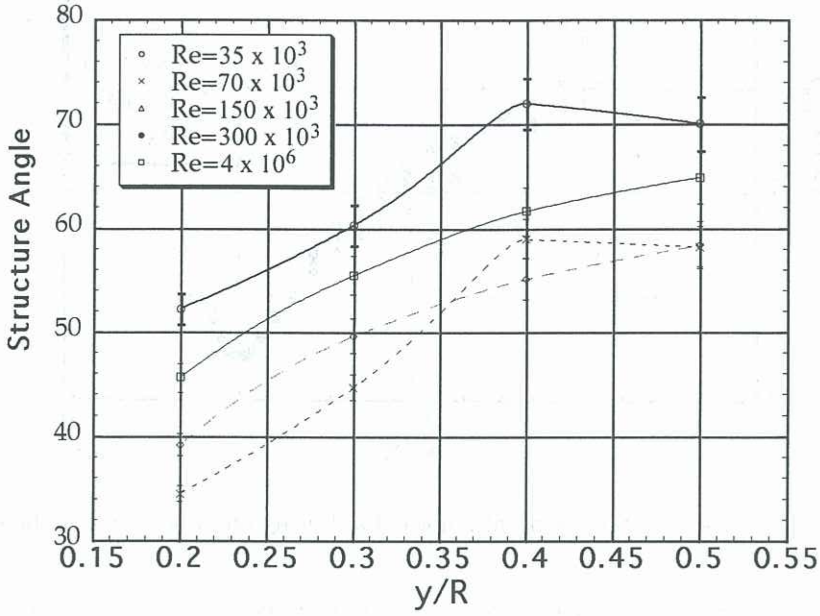

Figure 3: Structure angles (low to medium Reynolds numbers).

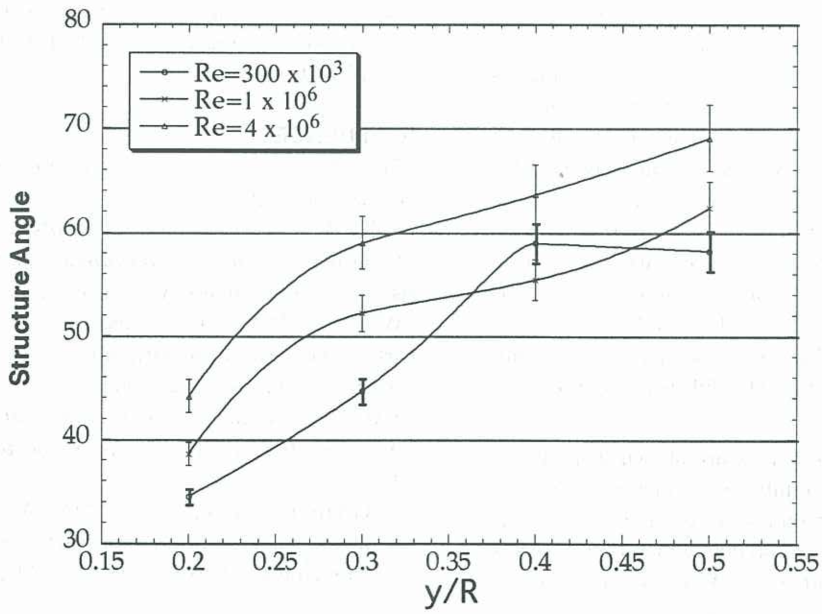

Figure 4: Structure angles (medium to high Reynolds numbers).